

Frequency dependence of the electrophoretic mobility for single colloids as measured using optical tweezers

Jun Ma,^{1,2} Tim Stangner,² and Friedrich Kremer²

¹*Hubei Collaborative Innovation Center for High-Efficiency Utilization of Solar Energy, School of Science, Hubei University of Technology, Wuhan 430068, China*

²*Institute of Experimental Physics I, Leipzig University, Linnéstrasse 5, D-04103 Leipzig, Germany*

(Received 18 July 2016; published 30 October 2017)

Optical tweezers accomplished with fast (100 μ s) particle tracking are employed to determine the frequency (1–1000 Hz) dependence of the electrophoretic mobility μ of a *single* colloid in an external oscillating electric (ac) field. The colloid under study is held in a microfluidic channel filled with monovalent or divalent salt (KCl and CaCl₂) solutions of varying concentrations (10⁻⁴ to 10⁻¹ molar), and its response to an external ac field is measured. A pronounced steplike frequency dependence of the single colloid electrophoretic mobility (SCE- μ) is observed with a plateau on the low-frequency side (1–100 Hz) and a corner frequency, f_c , which shifts with increasing concentration of the salt solution. The results are explained by considering the characteristic time needed for polarizing the electric double layer surrounding the colloidal particle under study.

DOI: [10.1103/PhysRevFluids.2.104306](https://doi.org/10.1103/PhysRevFluids.2.104306)

I. INTRODUCTION

The motion of a colloidal particle driven by an oscillating (ac) electric field has numerous applications in the self-assembly of particles [1–4] and for microfluidic devices [1,3,5,6]. Although it is widely used, its detailed mechanism is not well understood. The mobility of a colloidal particle, μ , is given [7] as

$$\mu = \frac{v}{E} = \frac{\varepsilon\zeta}{\eta}, \quad (1)$$

where ε and η are the permittivity and the dynamic viscosity of the liquid surrounding the colloid, respectively, v the drift velocity of the colloid, E the strength of electric field, and ζ the zeta potential. The particle mobility under the influence of an ac electric field is determined by the dielectric properties of the charged colloid surrounded by a double layer of counterions [8]. Its induced effective dipole moment is given by the relative permittivity of the particle and the electrolyte solution.

At high frequencies (typically MHz), the dispersion is characterized by the Maxwell-Wagner-O’Konski theory [8]. Classic models were proposed for the electrophoretic mobility of a colloidal particle [9,10] and further developed in subsequent studies [11,12]. These models successfully predict the decrease of the mobility at high frequencies [10]. Zhou *et al.* theoretically showed that the mobility of a colloidal particle displays a frequency dependence on an external electric field [13] inducing a polarization of the counterion double layer [14,15]. Considering the weak oscillating field as a small perturbation for the electrostatic field, the double layer is slightly distorted. This causes a frequency dependence of the mobility of the spherical particle as shown by Ohshima [16,17]. The mobility reduction of the colloidal particle was theoretically predicted [18] and experimentally observed at $\sim 10^7$ Hz [5].

At lower frequencies (kHz), Murtsookin and coworkers firstly suggested that polarizing the double layer results in an electro-osmotic flow [19,20]. Bazant and Squires further proposed the concept of induced-charge electro-osmosis (ICEO) to illustrate the flow resulting from the motion of the induced charge cloud surrounding the particle [6,21]. The broken symmetry of ICEO leads to the induced-charge electrophoresis, which drives the particle to move [6,21,22]. Grosse and Delgado classified the increase of the colloidal permittivity at frequencies in the kHz range as α -dispersion. It is caused

by counterion polarization, i.e., the concentration of ions increases near the surface of the particle. Then the ion motion in the double layer driven by the electric field produces the osmotic flow [8].

Optical tweezers have been employed in several “single-particle” experiments to study the electrophoretic mobility of (1) highly isolated charged [23] and (2) of electrostatically interacting colloidal spheres [24]; furthermore (3) they have been used as ultrasensitive tools to determine the effective charge of single particles [25] or to measure (4) the electrokinetic interactions and flow properties within microstructures [26]. Semenov *et al.* carried out experiments on the electrophoretic mobility and charge inversion of isolated colloidal particles [27–29]. To the best of our knowledge, the low-frequency (< 1 kHz) electrophoretic response has not been systematically studied in single colloidal particle experiments.

II. MATERIALS AND METHODS

A. Materials

Spherical polystyrene (PS) particles (Microparticles GmbH, Berlin, Germany, diameter: $2.23 \pm 0.05 \mu\text{m}$; polydispersity index: 0.05) in a 4% stock solution are used. Salt solutions are diluted by deionized water (Millipore water, $\text{pH} : 5.8$; conductivity: $5 \mu\text{S/m}$). The pH value is found to be stable during the measurement. The measurements are performed in aqueous solutions ($\text{pH} : 5.8$) of KCl and CaCl_2 .

B. Microfluidic cell

To perform our single colloid experiments we use a microfluidic flow cell consisting of a channel with rectangular cross-section (height 1 mm, width 0.3 mm) connecting two reservoirs (Fig. 1). The cell is made out of a micro-machined poly-methyl-met-acrylate spacer, enclosed between a microscope slide (thickness 1 mm) and a coverslip (thickness $160 \mu\text{m}$) at the top and the bottom, respectively, and sealed by UV-sensitive glue. Platinum electrodes are inserted into the two reservoirs. The particle is located either at the center (“A”) of the cross section of the channel or outside of the electrodes (“B”).

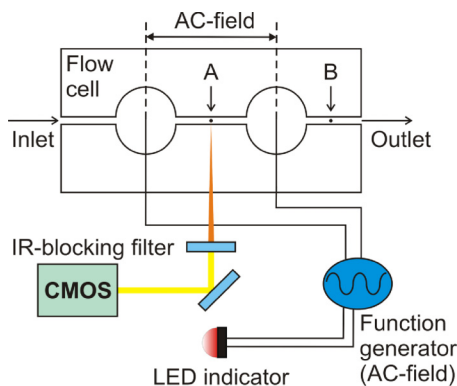


FIG. 1. Scheme of the experimental setup. The electrophoretic response of a single particle (diameter: $2.23 \mu\text{m}$) and the electroosmotic response of the surrounding medium are measured separately by placing the identical colloid in positions A and B, respectively. The ac oscillating electric field is applied to the colloid under study using platinum electrodes which are inserted into the reservoirs. For the colloid in position A, both the electrophoretic and the electroosmotic responses are superimposed, while in position B, no electric field is present and hence only the electroosmotic effect is observed. The inlet and outlet of the channel (width: 0.3 mm, height: 1 mm) are kept open to avoid any changes in the pressure inside the channel. The particle motion is traced by using an epifluorescence microscope equipped with a high-speed (10 000 frames/s) CMOS camera. Using a LED flash, the zero value of the external electric field is indicated in the sequence of the images.

C. Optical tweezers

Optical tweezers (OT) are an effective tool to study the electrophoresis of a *single* colloidal particle under the influence of an external oscillating electric field [27,28,30]. The amplitude of electrophoretic responses of different colloids displays reproducibility with an averaged standard deviation of $\sigma = 1.6$ nm [29]. The single particle is trapped by a focused $\lambda = 1064$ nm laser beam. This can be well approximated as a particle in a harmonic potential. Being proportional to the beam power, the force constant is 0.04 pN nm⁻¹ with the laser power of 0.2 W. The particle displacement is measured by a CMOS high-speed camera (10 000 fps) using diffraction pattern analysis [31]. The spatial resolution is ± 2 nm, corresponding to a resolution in force of ~ 160 fN. The zero value of the external ac electric field is indicated by a LED flash, which is recorded by the CMOS camera monitoring the movement of the colloid under study.

D. Measuring the electrophoretic mobility

To acquire the electrophoretic mobility μ of a particle, the bead is placed with the OT either at the position A or B , respectively. This corresponds to the measurements of the total complex electrokinetic response of the particle and the separate electroosmotic effect of the surrounding medium, respectively (Fig. 1). The amplitude (A_e) and the phase (φ_e) of the particle oscillations are given by

$$A_e e^{-i\varphi_e} = A_a e^{-i\varphi_a} + A_b e^{-i\varphi_b} \quad (2)$$

where A_a, A_b and φ_a, φ_b are the amplitudes and phases measured at positions A and B , respectively. A_e and φ_e can be described by an overdamped harmonic oscillator model [31]

$$A_e = \frac{\mu E}{\omega_c \sqrt{1 + (\omega/\omega_c)^2}}, \quad \varphi_e = \arctan \frac{\omega}{\omega_c} \quad (3)$$

where ω and ω_c are the frequency of the external electric field and the cutoff frequency of optical trap, respectively, and μ the electrophoretic mobility. Thus the mobility can be determined from the slope of the amplitude versus ac field strength. As we showed previously, the electrophoretic and the electroosmotic responses display a linear dependence on the strength of the external ac field, the latter being much weaker, and its phases are nearly independent on the strength of the external ac field [27–29]. To ensure that the particle motion caused by electrophoretic effects is not suppressed or distorted by the stall forces of the optical trap, we estimate the ratio between electrical and optical forces to be lower than 3% (see the Appendix). Based on this, restoring forces originating from the OT can be neglected in the analysis of the electrophoretic mobility μ .

E. Developing a theoretical model to describe the experimental data

In order to describe the frequency dependence of the electrophoretic mobility μ , we are now developing a theoretical model by considering the continuous formation and disintegration of double layer resulting from the direction reversal of the low-frequency ac field. Thus, here we study on the dynamic process of ions forming a double layer. First we consider an ion moving with the velocity v_i in the suspension. According to Stokes' law, the friction force enacting on the ion is [32]

$$f_d = \gamma v_i \quad (4)$$

with the friction coefficient $\gamma = 6\pi\eta r_i$ (r_i , ion radius).

Since a colloidal particle carries negative charge, the cations are accumulated near its surface. The motion of an ion is accelerated under the influence of an electric field until the electric force acting on the ion is balanced by the friction force, i.e., the ion reaches its maximum velocity v_0 ,

$$\gamma v_0 = 0.707eE \quad (5)$$

where e is the elementary charge. In electric engineering, as the time averaged value is adopted for the ac electric field, the root mean square (rms) value is used [33], i.e., $E/\sqrt{2} = 0.707E$, where E is the peak value of the field strength. Thus the maximum velocity (corresponding to the time averaged ac electric field) of the ion is

$$v_0 = 0.707eE/\gamma. \quad (6)$$

Manning pointed out that, counterions condense to form a polyion under the influence of an external electric field [15,34]. This is considered to occur near the surface carrying a high amount of charge [17]. More ions are accumulated in the double layer as the voltage is increased. For a high packing density, a condensed layer of ions is formed near the particle surface [35]. The double layer consists of both a compact and a diffuse layer [36].

We assume a charging zone (CZ) near a particle in the polarizing process. As the ions are accumulating, an osmotic pressure is produced with the direction pointing from the charging zone to the bulk suspension as [37]

$$P_0 = nk_B T \quad (7)$$

in which $n = n_{cz} - n_b$, n_{cz} and n_b are the ion number density of the charging zone and bulk suspension, respectively, and $k_B T$ is the thermal energy. This equation is an approximation from equation $P_0 = nk_B T(1 + B_2 n + \dots)$ (B_2 , the second virial coefficient) [38], as in the present work $B_2 n \leq 10^{-3} \ll 1$ holds.

Once the osmotic force acts on the ion, it can balance the effect of the external electric force,

$$P_0 s_i = 0.707eE \quad (8)$$

in which $s_i = \pi r_i^2$ is the projection area of an ion along the direction of osmotic pressure. At a certain point, the velocity of the ion damps to zero due to the friction force f_d . Thus the number density of ions reaches the saturation number density,

$$n_s = \frac{0.707eE}{k_B T s_i}. \quad (9)$$

As an ion driven by the electric field is approaching the charging zone, the osmotic force enacting on the ion is exponentially increased as

$$F_o = n_s k_B T s_i e^{-\beta_1(l-x)} \quad (10)$$

where β_1 is an exponential coefficient, l the initial distance between the ion and the charging zone, x the displacement of the ion. Since the osmotic force acting on the ion increases with increasing displacement, its velocity is damped when moving towards the charging zone:

$$v = v_0 e^{-\beta x} \quad (11)$$

where β is a damping coefficient. For the ion moving under the influence of the external electric field, its energy change with respect to the initial state ($x = 0$) is

$$0.707eEl - \int_0^l \gamma v dx - \int_0^l s_i n(x) k_B T e^{-\beta_1(l-x)} dx = \frac{1}{2} m v^2 - \frac{1}{2} m v_0^2 \quad (12)$$

where m is the ion mass. The quantity of the left side of the above mentioned equation is far larger than that of the right side,¹

$$0.707eEl - \int_0^l \gamma v_0 e^{-\beta x} dx - \int_0^l s_i n(x) k_B T e^{-\beta_1(l-x)} dx \approx 0. \quad (13)$$

As the ion is driven towards the charging zone, the increasing osmotic force leads to the damping of the ion velocity. Thus its velocity is gradually decreasing from the initial value v_0 . Applying Newton's second law, the equation of motion is

$$F_d = 0.707eE - f_d - F_o = ma \quad (14)$$

where F_d is the damping force and a the acceleration of the ion.

When an ion is moving towards the charging zone, the osmotic force acting on the ion increases with the time as

$$F_o = n_s(1 - e^{-\beta' t})k_B T s_i \quad (15)$$

where β' is a constant. The momentum change of the ion from the initial state is

$$0.707eEt_i - \int_0^{t_i} \gamma v dt - \int_0^{t_i} n_s(1 - e^{-\beta' t})k_B T s_i dt = mv - mv_0 \quad (16)$$

Similarly, it has²

$$0.707eEt_i - \int_0^{t_i} \gamma v dt - \int_0^{t_i} n_s(1 - e^{-\beta' t})k_B T s_i dt \approx 0. \quad (17)$$

After the calculation of Equation (17) (see the Appendix), one obtains for the charging time t_i

$$t_i = \frac{1.582\gamma\delta}{s_i n_b k_B T}. \quad (18)$$

The dynamical charging process can be represented as

$$\frac{Q}{S} = \int_0^t J dt \quad (19)$$

in which $J = en_b v$ [v given by Eq. (A4) in the Appendix] is the ion charge flux; $S = \pi r_p^2$ is the projection area of a colloidal particle (r_p colloidal particle radius) along the electric field direction and Q the colloid charge. Substituting the formula of J into Eq. (19), and performing the integration, delivers

$$Q = \pi r_p^2 en_b v_0 t_i (1 - e^{-\frac{t}{t_i}}). \quad (20)$$

The surface charge density, q_s , is given by the standard Poisson-Boltzmann model as [39]

$$q_s = 2\sqrt{2\epsilon k_B T n_b} \sinh\left(\frac{Ze\xi}{2k_B T}\right). \quad (21)$$

¹As the ions in the volume ($l \times$ unit area) are driven into a charging thickness δ , it has $l = n_s \delta / n_b$. Thus eEl can be calculated from the δ values in Table I. The work done by the electric field ($0.707eEl$) ranges from $\sim 10^{-26}$ to $\sim 10^{-23}$ J for the different concentrations used in the present work. With an initial (maximum) kinetic energy of the ion of $mv_0^2/2 = 8.5 \times 10^{-35}$ J, one finds $0.707eEl \gg mv_0^2/2$. Since the values of the other terms in left side of Eq. (12) are comparable to $0.707eEl$, with $v < v_0$, it has Eq. (13).

²For typical values of t_i from $\sim 10^{-5}$ to $\sim 10^{-2}$ s, $0.707eEt_i$ ranges from $\sim 10^{-22}$ to $\sim 10^{-18}$ kg · m · s⁻¹. With $mv_0 = 3.3 \times 10^{-30}$ kg · m · s⁻¹, $0.707eEt_i \gg mv_0$ holds. Due to $v < v_0$, it has Eq. (17).

Equation (21) can be written as $q_s = \sqrt{2\epsilon k_B T n_b} (e^{\frac{Ze\zeta}{2k_B T}} - e^{-\frac{Ze\zeta}{2k_B T}}) \approx \sqrt{2\epsilon k_B T n_b} e^{\frac{Ze\zeta}{2k_B T}}$ (with cations driven by the electric field considered here). As the effective area of the colloid, that is interacting with the electric field, follows from the Derjaguin approximation (see the Appendix [40]), its charge quantity can be considered as $Q = \pi r_p^2 \sqrt{2\epsilon k_B T n_b} e^{\frac{Ze\zeta}{2k_B T}}$. Therefore the expression for the zeta potential reads as

$$\zeta = \frac{2k_B T}{Ze} \ln \frac{Q}{\pi r_p^2 \sqrt{2\epsilon k_B T n_b}}. \quad (22)$$

Substituting Eq. (22) into Eq. (1), delivers the electrophoretic mobility as

$$\mu = \frac{2k_B T \epsilon}{Ze \eta} \ln \frac{Q}{\pi r_p^2 \sqrt{2\epsilon k_B T n_b}}. \quad (23)$$

By analyzing Eq. (20) by its time dependence, two different regimes can be distinguished. As $t \rightarrow \infty$ (corresponding to $f \rightarrow 0$), the mobility of the colloid can be considered to correspond to the condition under a direct current (dc) electric field, hence Eq. (20) turns into

$$Q_{dc} = \pi r_p^2 \epsilon n_b v_0 t_i. \quad (24)$$

For a unit area with the charging time t_i , $n_b l$ ions have been driven into the charging zone by the electric field. The cations in the charging zone further accumulate near the negative charged surface of the colloidal particle and form a condensed layer. Thus the area density of the charge of the double layer is $n_b l$. The length l , is determined by the charge quantity in the double layer, thus l is the characteristic parameter of the system, being related with t_i through Eqs. (13) and (17). When the charge quantity Q , in Eq. (23) is given by the Q_{dc} under the influence of a dc field in Eq. (24), the mobility of a colloidal particle is constant.

However, if $t \rightarrow 0$ (corresponding to $f \rightarrow \infty$) the colloid response is caused by an ac electric field with frequency f , in which the polarizing zone can be fully developed if $t_i > \frac{1}{2f}$ [41]. In this limit, the charge Q is given by Eq. (20) and allows us to predict the reduction in the electrophoretic mobility. Additionally, it was pointed out that forming the polarizing zone is analogue to charging a RC circuit [6,41–44] with a double-layer “capacitor” [6,36,43,44]. This is described by

$$Q_c(t) = Q_0 (1 - e^{-\frac{t}{\tau}}) \quad (25)$$

where $Q_c(t)$ is the time dependent charge, Q_0 is the charge for $t \rightarrow \infty$, and τ is the time constant of the system. Substituting Eq. (24) into Eq. (20), delivers

$$Q(t) = Q_{dc} (1 - e^{-\frac{t}{\tau}}). \quad (26)$$

In contrast, for an ac electrical field it is known that using only t_i in Eq. (20) leads to an underestimation of the charge Q . In this case the time constant of the system in Eq. (20) consists of the charging time (t_i) and the time (t_d) for developing a more condensed CZ zone. As indicated by Bazant *et al.*, counterions near the charged surface turn into a crowded state under the influence of the electric field [45]. Therefore, the whole process can be understood as follows: ions are driven into the charging zone and finally accumulate to form the condensed charge zone, hence the time $t_s (= t_i + t_d)$ has to be taken instead of t_i in Eq. (20). By replacing the time t_i with t_s and substituting Eqs. (18) and (20) into Eq. (23) one finds for the mobility

$$\mu = \frac{2k_B T \epsilon}{Ze \eta} \ln \left[\frac{0.252 e^2 E \delta}{(\epsilon n_b)^{\frac{1}{2}} (k_B T)^{\frac{3}{2}} r_i^2} (1 - e^{-\frac{f_c}{f}}) \right] \quad (27)$$

where f_c is the corner frequency corresponding to the characteristic time constant t_s , f the frequency of the ac electric field. δ is the charging thickness with the saturation number density, n_s , defined by Eq. (9).

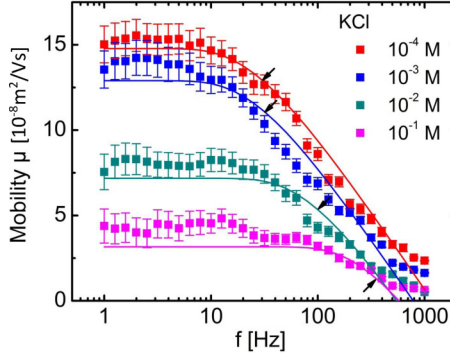


FIG. 2. Frequency dependence of the single-particle electrophoretic mobility in KCl solution of varying concentrations as indicated. The solid lines are fits with the proposed model [see Eq. (27)]. In the low-frequency range ($f \leq 100$ Hz) μ stays almost constant. After exceeding a certain frequency (f_c , black arrows, Table I), the electrophoretic mobility decreases. Error bars indicate the standard deviation of the data.

III. RESULTS AND DISCUSSION

In order to validate the proposed model we measure the electrophoretic mobility μ in dependence of an alternating electrical field with frequency f , in solutions with ion valance and ion concentration (Figs. 2 and 3), respectively.

For the particle motion driven by the ac electric field in KCl solution, the electrophoretic mobility μ of the particle stays almost constant for frequencies below 100 Hz, resulting in a flat platform. After exceeding a distinct corner frequency f_c , μ starts to decrease. In common sense, f_c refers to a boundary in the frequency response of the system, at which the characteristic parameter of the system begins to reduce [46]. Here we denote the corner frequency as a frequency at which mobility reduction starts, as indicated by the arrows in Figs. 2 and 3. As the KCl concentration is increased from 10^{-4} to 10^{-1} M, f_c significantly grows, whereas the plateau value of the particle mobility decreases from $\sim 14.8 \times 10^{-8}$ to $\sim 3.2 \times 10^{-8}$ m²/Vs. The increase of f_c is based on the fact that for high salt concentrations the time needed for charging the polarizing zone is shortened. As we observed previously, the phase angle of particle motion remains almost unchanged with increasing KCl concentration (10^{-4} – 10^{-1} M) and ac frequency (1–1000 Hz) [29]. The observed absolute values for particle mobility at the plateau in Fig. 2 are close to values reported in other

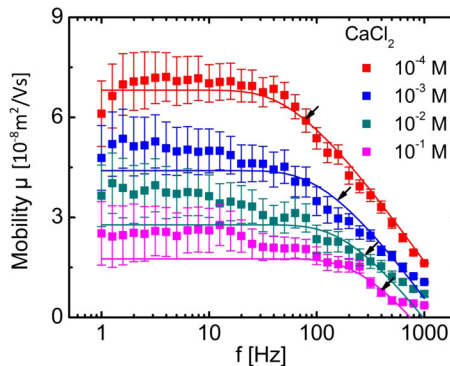


FIG. 3. Frequency dependence of the single-particle electrophoretic mobility in CaCl₂ solution of varying concentration as indicated. The solid lines are fits with the proposed model [see Eq. (27)]. We observe the same trend as for KCl. Error bars indicate the standard deviation of the data.

TABLE I. The parameters δ and f_c are obtained fitting the data in Figs. 2 and 3 using Eq. (27).

Solvent	Parameter	10^{-4} M	10^{-3} M	10^{-2} M	10^{-1} M
KCl	δ (nm)	197 ± 4	389 ± 8	295 ± 6	342 ± 7
	f_c (Hz)	30 ± 1	32 ± 2	100 ± 5	350 ± 17
CaCl ₂	δ (nm)	82 ± 2	78 ± 2	109 ± 2	207 ± 4
	f_c (Hz)	80 ± 4	160 ± 8	280 ± 14	400 ± 20

studies, e.g., investigating the mobility of PS particles under a dc electric field: $5.6 \times 10^{-8} \text{ m}^2/(\text{sV})$ in 10^{-2} M KBr [47] and $5.9 \times 10^{-8} \text{ m}^2/(\text{sV})$ in 10^{-2} M KCl [48].

For the single-particle electrophoretic mobility in a divalent salt (CaCl₂) solution of varying concentration, the results are similar with those in KCl solution (Fig. 3). However, for the same concentration, the particle mobility in the CaCl₂ solution is lower than that in the KCl solution. As the CaCl₂ concentration is growing from 10^{-4} to 10^{-1} M, the particle mobility corresponding to the low-frequency platform (< 100 Hz) decreases from $\sim 6.8 \times 10^{-8}$ to $\sim 1.8 \times 10^{-8} \text{ m}^2/\text{Vs}$, whereas the corner frequency f_c , rises to several hundred Hertz (Fig. 3, black arrows, Table I). These are consistent with other studies: Kahl *et al.* observed that the mobility of a charged microsphere trapped in an optical tweezer decays under ac field at 400 Hz [26], and Ma *et al.* experimentally found that the mobility of polystyrene dimer decreases from 300 Hz [49]. The phase angle of particle motion keeps a constant value at low frequency ($1 \sim 40$ Hz) and increases slightly afterwards at higher frequencies (data not shown).

We now use Eq. (27) to fit the experimental results.³ Figures 2 and 3 show that both experimental results and theoretical predictions display the mobility reduction of a colloid in an ac electric field with increasing frequency. Additionally, by substituting Eqs. (18) and (24) into Eq. (22), we can derive further characteristic system parameter such as charging thickness δ (Table I) and zeta potentials ζ (Fig. 4).

For salt concentrations between 10^{-4} M and 10^{-1} M, ζ ranges from 41 mV to 190 mV (KCl) and from 22 mV to 87 mV (CaCl₂), respectively. Figure 4 shows a tendency that the zeta potential ζ decreases with both concentrations of KCl and CaCl₂ increasing, which agrees with the result reported before [45]. Moreover, the zeta potential ζ of divalent salt of CaCl₂ is lower than that of monovalent salt of KCl, which is also consistent with the fact that the higher valency electrolytes more effectively screen the electric potential than that of the lower one [39]. From Fig. 4 and Eq. (1), the mobility of colloidal particle decays with the salt concentration and electrolyte valency increasing, which agrees with the mobility change shown in Figs. 2 and 3.

The obtained ζ values are in the same order of magnitude as they were observed by other electrokinetic measurements for colloidal particles: 130 mV in 1.6×10^{-4} M KCl [50], 100 mV in 10^{-3} M KCl [51], and 30 mV in 2×10^{-2} M CaCl₂ + Ca(OH)₂ [52]. Despite deviations of up to 40%, the agreement of our ζ values and those published in literature is reasonable by considering different experimental conditions.

However, for frequencies below 100 Hz the fits in Figs. 2 and 3 slightly underestimate our experimental data. This may be attributed to the following reasons: the very low frequencies of the plateau are located in a transient frequency regime between the dc electric field and the ac one. Although the feature of ac field dominates the particle mobility but that of the dc field also plays a

³Since the experiments are conducted under the electric field in a range from 1 V/cm to 18 V/cm, here we choose the median value 9.5 V/cm for fitting the experimental data. Varying the voltage in the above range does not affect the mobility: using the continuity equation for ions, $n_b l = n_s \delta$ and combining it with Eqs. (7) and (8) results in $E \delta = \pi r_i^2 k_B T n_b l / 0.707 e$. Because all parameters on the right side of equation are constant, $E \delta$ keeps constant. Thus from Eq. (27) the mobility is unchanged.

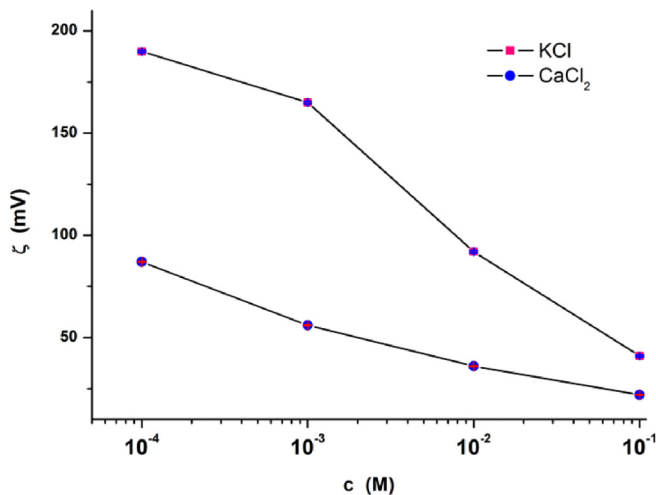


FIG. 4. Zeta potential ζ calculated from Eq. (22) [and Eqs. (18) and (24)] for the monovalent salt KCl (pink squares) and the divalent salt CaCl_2 (blue circles). As can be seen, ζ decreases with increasing salt concentration for both salts. The error bars for KCl and CaCl_2 solutions are ± 0.51 mV and ± 0.25 mV, respectively, represented by the error bars enclosed in the (circle or square) symbols.

perturbative role. The theoretical model in the present work mainly captures the characteristics of particle mobility in the ac one, but the diminutive feature of dc electric field is ignored, thus the fits do not precisely coincide with the plateau at the low-frequency side.

In addition, at low frequencies electrode polarization occurs which is not considered in our theoretical model. In order to estimate the impact of such effects, we calculate the dimensionless number $\omega L/D\kappa$ (with $\omega = 2\pi f$ frequency, L the distance between the electrodes, D the diffusion coefficient of the ions, and $1/\kappa$ the Debye length). Only when this number is larger than about 5, electrode polarization can be neglected (see the Appendix). For a given salt concentration, this gives the minimum frequency below which electrode polarization has to be considered. As can be seen from Table II, electrode polarization becomes important for frequencies (< 100 Hz), providing an explanation why our model underestimates the data in this frequency range.

IV. SUMMARY

A setup based on optical tweezers is employed to carry out electrophoretic measurements with isolated single colloids (single colloid electrophoresis) being held in a microfluidic channel. Colloid mobility dependence is studied with the various parameters, such as strength (1–15 V/cm) and frequency (1 Hz to 1000 Hz) of the external ac field, ion concentration (10^{-4} to 10^{-1} M), and ionic valence (KCl and CaCl_2) of the solution. A pronounced frequency dependence is observed for the

TABLE II. Salt-dependent frequency below which the dimensionless number $\omega L/D\kappa$ becomes smaller than 5 and thus electrode polarization effects have to be considered.

c (M)	$\omega L/D\kappa$ for Na^+ and Cl^- ions (Hz)	$\omega L/D\kappa$ for Ca^{2+} ions (Hz)
10^{-4}	≤ 2	≤ 3
10^{-3}	≤ 5	≤ 7
10^{-2}	≤ 24	≤ 30
10^{-1}	≤ 44	≤ 61

electrophoretic mobility μ with a plateau on the low-frequency side ($f < 100$ Hz) and a steplike decline at a corner frequency f_c .

The current theory successfully predicts multiple aspects of the experimental results: (1) the frequency dependence of the colloidal mobility; (2) the plateau on the low-frequency side; (3) a steplike decline at the corner frequency f_c ; (4) the mobility decreasing with salt concentration increasing; (5) the low-frequency plateau extended with increasing salt concentration to the higher frequencies; (6) the colloidal mobility decreasing as the valence of salt (KCl, CaCl₂) increases. The results can be quantitatively comprehended considering the time dependence of charging the electric double layer covering the colloid under study.

ACKNOWLEDGMENTS

We thank Ilya Semenov for carrying out the experiments and Professor Hiroyuki Ohshima for critical comments on the manuscript. Support of the German Science Foundation (DFG) within the SFB-TRR 102 is gratefully acknowledged.

APPENDIX

We calculate the electrical force using $F_{el} = qE = Z_{DLVO}eE$, where Z_{DLVO} is the effective colloid surface charge (average values for KCl and CaCl₂ taken from Ref. [53]; Table I) and E the electric field (values taken from Ref. [29]; Fig. 2). The stall force of the optical tweezers is determined by Hook's law: $F_{Stall} = k\Delta x$, with k being the trap stiffness and Δx the displacement of the colloid from its equilibrium position caused by the electrical field (values taken from Ref. [29]; Fig. 2). The ratio between F_{Stall}/F_{el} is approximately 2% for KCl and 3% for CaCl₂ showing that effects originating from the optical tweezers on the electrophoretic motion of the bead can be neglected.

Now we derive the relation among the forces acting on the ion. Supposing only the initial friction force acting on the potassium ion with the velocity v_0 , the time for reducing the momentum of the ion to zero is $t_f = \frac{mv_0}{\gamma} = \frac{m}{\gamma} = 2.6 \times 10^{-14}$ s. As t_i ($\sim 10^{-5}$ to $\sim 10^{-2}$ s) is much larger than t_f , the actual damping force F_d acting on the ion is much smaller than the initial friction force, $\frac{F_d}{\gamma v_0} \approx \frac{t_f}{t_i} \sim 10^{-12} - 10^{-9}$. Thus, from Eqs. (5) and (14), we have $0.707eE \gg F_d (=ma)$. In Eq. (14) f_d and F_o are the forces with the comparable magnitude of $0.707eE$, and thus we get

$$0.707eE \approx f_d + F_o. \quad (\text{A1})$$

Therefore, the external forces enacted on the ion are approximately balanced. In the process of the ion approaching the charging zone with decreasing velocity, Eq. (4) indicates that the friction force (f_d) is decreasing. In contrast, the osmotic force is increasing. As indicated by Eqs. (4), (10), and (11), $f_d \propto e^{-\beta x}$, $F_o \propto e^{-\beta_1(l-x)} = e^{-\beta_1 l} e^{\beta_1 x} = C e^{\beta_1 x}$, in which $C = e^{-\beta_1 l}$ is a constant, and β and β_1 are damping and growth coefficients for f and F_o , respectively. To meet the condition of force balance in Eq. (A1), the decreasing amount of f_d should be equal to the increasing amount of F_o . Thus one finds $\beta_1 \approx \beta$. From Eq. (13), one obtains

$$0.707eEl - \int_0^l \gamma v_0 e^{-\beta x} dx - \int_0^l s_i n(x) k_B T e^{-\beta(l-x)} dx = 0. \quad (\text{A2})$$

As the number of ions is kept constant, ions within the displacement length x (corresponding to the volume: x -unit area) contribute to those in a charging thickness δ (corresponding to the volume: δ -unit area), thus $n_b x = n(x)\delta$. Substituting $n(x)$ and Eqs (5), (7), and (8) into Eq. (A2), and performing the integration, one obtains

$$(\beta l - 1)^2 + (\beta l - 1)e^{-\beta l} = 0. \quad (\text{A3})$$

Thus $\beta l = 1$. The damping of the ion velocity with time can be represented as

$$v = v_0 e^{-\beta' t} \quad (\text{A4})$$

where β' is a damping coefficient. As the ion displacement l [Eq. (11)] corresponds to the time t_i , it has to obey the boundary condition: $e^{-\beta l} = e^{-\beta' t_i}$. Thus $\beta' t_i = \beta l = 1$, i.e., $\beta' = \frac{1}{t_i}$.

With $l = \int_0^{t_i} v dt$, $\beta' = \frac{1}{t_i}$, $n_s = n_b l / \delta$ and Eqs. (5), (7), and (8), one obtains t_i [Eq. (18)] from Eq. (17).

Derjaguin approximation is widely used to calculate the interaction energy acting on a spherical surface [40]. In Derjaguin approximation, the spherical surface is considered to consist of a series of infinite small area dS . As the normal (n) of dS possesses an angle to the external field E , dS corresponds to the effective area dS' (its normal n' parallel to E) interacting with E . The whole effective interaction area in an external field is constituted of a series of infinite small areas like dS' . Thus the effective area of the half spherical surface of colloidal particle in the field E is πr^2 .

In order to estimate the effect of electrode polarization, we calculate the dimensionless number $\omega L / D\kappa$, with $\omega = 2\pi f$ being the frequency and $1/\kappa$ the Debye length. The ion diffusion constant D can be determined by using Fick's first law [54]:

$$D = \frac{\mu k_B T}{Ze}, \quad (\text{A5})$$

with μ is the ion mobility at room temperature at an electrical field strength of 1 V/m, $k_B T$ the thermal energy, and Ze the charge of the ion. Equation (A5) results in the following ion diffusion coefficients: $D_{K^+} = 1.95 \times 10^{-9} \text{ m}^2/\text{s}$, $D_{Ca^{2+}} = 7.92 \times 10^{-10} \text{ m}^2/\text{s}$, and $D_{Cl^-} = 2.03 \times 10^{-9} \text{ m}^2/\text{s}$ [55]. L is the distance between the electrodes and is given by $L = 40 \text{ mm}$. For $\omega L / D\kappa < 5$ electrode polarization has to be considered. The respective threshold frequencies can be found in Table II.

-
- [1] O. D. Velev and K. H. Bhatt, On-chip micromanipulation and assembly of colloidal particles by electric fields, *Soft Matter* **2**, 738 (2006).
 - [2] J. J. Juarez, P. P. Mathai, J. A. Liddle, and M. A. Bevan, Multiple electrokinetic actuators for feedback control of colloidal crystal size, *Lab Chip* **12**, 4063 (2012).
 - [3] S. Kim, R. Asmatulu, H. L. Marcus, and F. Papadimitrakopoulos, Dielectrophoretic assembly of grain-boundary-free 2D colloidal single crystals, *J. Colloid Interface Sci.* **354**, 448 (2011).
 - [4] M. Mittal and E. M. Furst, Electric field-directed convective assembly of ellipsoidal colloidal particles to create optically and mechanically anisotropic thin films, *Adv. Funct. Mater.* **19**, 3271 (2009).
 - [5] J. A. van Heiningen, A. Mohammadi, and R. J. Hill, Dynamic electrical response of colloidal micro-spheres in compliant micro-channels from optical tweezers velocimetry, *Lab Chip* **10**, 1907 (2010).
 - [6] M. Z. Bazant and T. M. Squires, Induced-Charge Electrokinetic Phenomena: Theory and Microfluidic Applications, *Phys. Rev. Lett.* **92**, 066101 (2004).
 - [7] M. V. Smoluchowski, Versuch einer mathematischen Theorie der Koagulationskinetik kolloidaler Lösungen, *Z. Physik Chem.* **92**, 129 (1917).
 - [8] C. Grosse and A. V. Delgado, Dielectric dispersion in aqueous colloidal systems, *Curr. Opin. Colloid Interface Sci.* **15**, 145 (2010).
 - [9] R. W. O'Brien and L. R. White, Electrophoretic mobility of a spherical colloidal particle, *J. Chem. Soc. Faraday Trans. II* **74**, 1607 (1978).
 - [10] C. S. Mangelsdorf and L. R. White, Electrophoretic mobility of a spherical colloidal particle in an oscillating electric field, *J. Chem. Soc., Faraday Trans.* **88**, 3567 (1992).
 - [11] R. J. Hill and D. Saville, 'Exact' solutions of the full electrokinetic model for soft spherical colloids: Electrophoretic mobility, *Colloids Surf. A* **267**, 31 (2005).
 - [12] R. J. Hill, D. Saville, and W. Russel, Polarizability and complex conductivity of dilute suspensions of spherical colloidal particles with uncharged (neutral) polymer coatings, *J. Colloid Interface Sci.* **268**, 230 (2003).

- [13] J. Zhou, R. Schmitz, B. Dünweg, and F. Schmid, Dynamic and dielectric response of charged colloids in electrolyte solutions to external electric fields, *J. Chem. Phys.* **139**, 024901 (2013).
- [14] J. K. Dhont and K. Kang, Electric-field-induced polarization and interactions of uncharged colloids in salt solutions, *Eur. Phys. J. E Soft Matter* **33**, 51 (2010).
- [15] G. S. Manning, Limiting laws and counterion condensation in polyelectrolyte solutions: V. Further development of the chemical model, *Biophys. Chem.* **9**, 65 (1978).
- [16] H. Ohshima, Dynamic electrophoretic mobility of a spherical colloidal particle, *J. Colloid Interface Sci.* **179**, 431 (1996).
- [17] H. Ohshima, Dynamic electrophoretic mobility of spherical colloidal particles in a salt-free medium, *J. Colloid Interface Sci.* **265**, 422 (2003).
- [18] V. N. Shilov, A. V. Delgado, F. González-Caballero, J. Horno, J. J. López-García, and C. Grosse, Polarization of the electrical double layer. Time evolution after application of an electric field, *J. Colloid Interface Sci.* **232**, 141 (2000).
- [19] N. I. Gamayunov, V. A. Murtsokin, and A. S. Dukhin, Pair interaction of particles in electric-field. 1. Features of hydrodynamic interaction of polarized particles, *Colloid J. USSR* **48**, 197 (1986).
- [20] V. A. Murtsokin, *Colloid J.* **58**, 341 (1996).
- [21] T. M. Squires and M. Z. Bazant, Breaking symmetries in induced-charge electro-osmosis and electrophoresis, *J. Fluid Mech.* **560**, 65 (2006).
- [22] S. Gangwal, O. J. Cayre, M. Z. Bazant, and O. D. Velev, Induced-Charge Electrophoresis of Metallo-dielectric Particles, *Phys. Rev. Lett.* **100**, 058302 (2008).
- [23] N. Garbow, M. Evers, and T. Palberg, Optical tweezing electrophoresis of isolated, highly charged colloidal spheres, *Colloids Surf. A* **195**, 227 (2001).
- [24] N. Garbow, M. Evers, T. Palberg, and T. Okubo, On the electrophoretic mobility of isolated colloidal spheres, *J. Phys.: Condens. Matter* **16**, 3835 (2004).
- [25] G. Seth Roberts, T. A. Wood, W. J. Frith, and P. Bartlett, Direct measurement of the effective charge in nonpolar suspensions by optical tracking of single particles, *J. Chem. Phys.* **126**, 194503 (2007).
- [26] V. Kahl, A. Gansen, R. Galneder, and J. O. Rädler, Microelectrophoresis in a laser trap: A platform for measuring electrokinetic interactions and flow properties within microstructures, *Rev. Sci. Instrum.* **80**, 073704 (2009).
- [27] I. Semenov, O. Otto, G. Stober, P. Papadopoulos, U. F. Keyser, and F. Kremer, Single colloid electrophoresis, *J. Colloid Interface Sci.* **337**, 260 (2009).
- [28] I. Semenov, P. Papadopoulos, G. Stober, and F. Kremer, Ionic concentration- and pH-dependent electrophoretic mobility as studied by single colloid electrophoresis, *J. Phys.: Condens. Matter* **22**, 494109 (2010).
- [29] I. Semenov, S. Raafatnia, M. Sega, V. Lobaskin, C. Holm, and F. Kremer, Electrophoretic mobility and charge inversion of a colloidal particle studied by single-colloid electrophoresis and molecular dynamics simulations, *Phys. Rev. E* **87**, 022302 (2013).
- [30] T. A. Wood, G. S. Roberts, S. Eaimkhong, and P. Bartlett, Characterization of microparticles with driven optical tweezers, *Faraday Discuss.* **137**, 319 (2008).
- [31] O. Ueberschär, C. Wagner, T. Stangner, C. Gutsche, and F. Kremer, A novel video-based microsphere localization algorithm for low contrast silica particles under white light illumination, *Opt. Lasers Eng.* **50**, 423 (2012).
- [32] E. Gonick, Stokes' law and the limiting conductance of organic ions, *J. Phys. Chem.* **50**, 291 (1946).
- [33] B. Grob, *Direct and Alternating Current Circuits: A Conventional Current Version* (McGraw-Hill, New York, 1986).
- [34] G. S. Manning, Limiting laws and counterion condensation in polyelectrolyte solutions. I. Colligative properties, *J. Chem. Phys.* **51**, 924 (1969).
- [35] B. D. Storey, L. R. Edwards, M. S. Kilic, and M. Z. Bazant, Steric effects on ac electro-osmosis in dilute electrolytes, *Phys. Rev. E* **77**, 036317 (2008).
- [36] A. A. Kornyshev, Double-layer in ionic liquids: Paradigm change?, *J. Phys. Chem. B* **111**, 5545 (2007).
- [37] J. N. Israelachvili, *Intermolecular and Surface Forces* (Academic Press, London, 1992).

- [38] H. N. Lekkerkerker and R. Tuinier, *Colloids and the Depletion Interaction*, Vol. 833 (Springer, New York, 2011).
- [39] J. H. Masliyah and S. Bhattacharjee, *Electrokinetic and Colloid Transport Phenomena* (John Wiley & Sons, New York, 2006).
- [40] V. A. Parsegian, *Van der Waals Forces: A Handbook for Biologists, Chemists, Engineers, and Physicists* (Cambridge University Press, Cambridge, 2005).
- [41] M. S. Kilic, M. Z. Bazant, and A. Ajdari, Steric effects in the dynamics of electrolytes at large applied voltages. I. Double-layer charging, *Phys. Rev. E* **75**, 021502 (2007).
- [42] M. Z. Bazant, K. Thornton, and A. Ajdari, Diffuse-charge dynamics in electrochemical systems, *Phys. Rev. E* **70**, 021506 (2004).
- [43] G. Pesce, V. Lisbino, G. Rusciano, and A. Sasso, Optical manipulation of charged microparticles in polar fluids, *Electrophoresis* **34**, 3141 (2013).
- [44] L. H. Olesen, H. Bruus, and A. Ajdari, AC electrokinetic micropumps: The effect of geometrical confinement, Faradaic current injection, and nonlinear surface capacitance, *Phys. Rev. E* **73**, 056313 (2006).
- [45] M. Z. Bazant, M. S. Kilic, B. D. Storey, and A. Ajdari, Towards an understanding of induced-charge electrokinetics at large applied voltages in concentrated solutions, *Adv. Colloid Interface Sci.* **152**, 48 (2009).
- [46] A. Godse and U. Bakshi, *Electronic Devices and Circuits* (Technical Publications, Pune, 2009).
- [47] R. Hidalgo-Alvarez, F. J. de las Nieves, A. J. Van der Linde, and B. H. Bijsterbosch, Conformational changes of polyglutamic acid adsorbed on cationic polystyrene as characterized by microelectrophoresis technique, *Colloid. Polym. Sci.* **267**, 853 (1989).
- [48] M. Elimelech and C. R. O'Melia, Effect of electrolyte type on the electrophoretic mobility of polystyrene latex colloids, *Colloids Surf.* **44**, 165 (1990).
- [49] F. Ma, X. Yang, H. Zhao, and N. Wu, Inducing Propulsion of Colloidal Dimers by Breaking the Symmetry in Electrohydrodynamic Flow, *Phys. Rev. Lett.* **115**, 208302 (2015).
- [50] N. G. Green, A. Ramos, A. González, H. Morgan, and A. Castellanos, Fluid flow induced by nonuniform ac electric fields in electrolytes on microelectrodes. I. Experimental measurements, *Phys. Rev. E* **61**, 4011 (2000).
- [51] J. A. Levitan, S. Devasenathipathy, V. Studer, Y. Ben, T. Thorsen, T. M. Squires, and M. Z. Bazant, Experimental observation of induced-charge electro-osmosis around a metal wire in a microchannel, *Colloids Surf. A* **267**, 122 (2005).
- [52] C. Labbez, A. Nonat, I. Pochard, and B. Jönsson, Experimental and theoretical evidence of overcharging of calcium silicate hydrate, *J. Colloid Interface Sci.* **309**, 303 (2007).
- [53] C. Gutsche, U. F. Keyser, K. Kegler, F. Kremer, and P. Linse, Forces between single pairs of charged colloids in aqueous salt solutions, *Phys. Rev. E* **76**, 031403 (2007).
- [54] A. Fick, Ueber diffusion, *Ann. Phys.* **170**, 59 (1855).
- [55] E. Samson, J. Marchand, and K. A. Snyder, Calculation of ionic diffusion coefficients on the basis of migration test results, *Mater. Struct.* **36**, 156 (2003).